Effects of Ligand Binding and Oxidation on Hinge-Bending Motions in *S*-Adenosyl-L-homocysteine Hydrolase

Mengmeng Wang, Jay R. Unruh, Carey K. Johnson, Krzysztof Kuczera,* Richard L. Schowen, and Ronald T. Borchardt

Departments of Chemistry, Molecular Biosciences, and Pharmaceutical Chemistry, The University of Kansas, Lawrence, Kansas 66045

Received November 10, 2005; Revised Manuscript Received March 24, 2006

ABSTRACT: Domain motions of *S*-adenosyl-L-homocysteine (AdoHcy) hydrolase have been detected by time-resolved fluorescence anisotropy measurements. Time constants for reorientational motions in the native enzyme were compared with those for enzymes where key residues were altered by site-directed mutation. Mutations M351P, H353A, and P354A were selected in a hinge region for motion between the open and closed forms of the enzyme, as identified in a previous normal-mode study [Wang et al. (2005) Domain motions and the open-to-closed conformational transition of an enzyme: A normal-mode analysis of *S*-adenosyl-L-homocysteine hydrolase, *Biochemistry 44*, 7228−7239]. In wild-type, substrate-free AdoHcy hydrolase (NAD^+ cofactor in each subunit), reorientational motions were detected on time scales of 10−20 and 80−90 ns. The faster motion is attributed to the domain motion, and the slower motion is attributed to the tumbling of the enzyme. The domain motion was also detected for the enzyme complexes E(NADH/3′-keto-adenosine) and E(NAD^+/3′-deoxyadenosine) but was absent for the complex E(NADH/3′-keto-neplanocin A). The results indicate that AdoHcy hydrolase exists in equilibrium of open and closed structures, with the equilibrium shifted toward the more mobile open form for the substrate-free enzyme, E(NAD^+), and for intermediates formed early in the catalytic cycle after substrate binding or formed late prior to product release, E(NAD^+/ligand). However, the strong inhibitor neplanocin A upon binding undergoes oxidation, forming the complex E(NADH/3′-keto-neplanocin). For this complex, which is analogous to the enzyme complex with the central catalytic intermediate, the equilibrium was shifted toward the more rigid closed form. A similar pattern was observed for M351P and P354A mutants. In contrast, the domain motion could not be detected, either in the absence or presence of ligands or with the cofactor in either the oxidized or reduced state, for the H353A protein, suggesting that this mutation changes the hinge-bending dynamics of the enzyme.

S-Adenosyl-L-homocysteine (AdoHcy)[1] hydrolase (EC 3.3.1.1) is a crucial enzyme involved in controlling transmethylation reactions (*1*) (Figure 1). Because its metabolic role makes it a promising target for the design of antiparasitic and antiviral drugs, understanding the mechanism of catalytic activity of AdoHcy hydrolase is an important goal. An intriguing feature of AdoHcy hydrolase is the presence of large-scale domain motion, confirmed by both experimental (*2*) and computational (*3*) studies.

Crystal structures of AdoHcy hydrolase (Figure 2) show that the tetrameric enzyme exists in the open form in the absence of the substrate (*4*), while enzyme−inhibitor complexes take on the closed form (*5*). The main difference between the open and closed structures (parts B and C of Figure 2) involves a hinge-bending motion, in which the substrate-binding domain reorients by about 18° relative to the cofactor-binding domain within each subunit of the homotetramer (*6*). This reorientation closes a surface cleft, isolating the inhibitor from the solvent, while the internal structures of the two large domains remain essentially unchanged. The crystal structures suggest the existence of two hinge regions between the moving domains, involving residues 182−196 (hinge region 1, HR1) and residues 352−356 (hinge region 2, HR2). Further experimental support for the existence of hinge-bending motions comes from fluorescence depolarization studies (*7*), which demonstrated that in the open form AdoHcy hydrolase undergoes large amplitude reorientations of the substrate-binding domain with a frequency of about 25 ns, which cease upon inhibitor binding.

Recently, we have performed a normal-mode analysis of low-frequency collective motions of AdoHcy hydrolase (*3*). Our results showed that in the open, substrate-free, form the protein undergoes hinge-bending motions along a direction that would carry the open form into the closed form, with motions in each of the four subunits occurring independently of one another and of other protein vibrations. Thus, the mechanical properties of the open structure induce the

* To whom correspondence should be addressed: Departments of Chemistry and Molecular Biosciences, University of Kansas, 1251 Wescoe Hall Drive, Lawrence, KS 66045. Telephone: 785-864-5060. Fax: 785-864-5396. E-mail: kkuczera@ku.edu.

[1] Abbreviations: Ado, adenosine; Hcy, homocysteine; AdoHcy, *S*-adenosyl-L-homocysteine; NAD^+ and NADH, oxidized and reduced forms of nicotinamide adenine dinucleotide; 3′-deoxyAdo, 3′-deoxyadenosine; 3′-ketoAdo, 3′-ketoadenosine; NepA, neplanocin A; DTNB, 5,5′-dithiobis-2-nitrobenzoic acid; DTT, dithiothreitol; PMal, *N*-(1-pyrenyl)maleimide; EDTA, ethylenediaminetetraacetic acid; WT, wild type; HR1, hinge region 1; HR2, hinge region 2.

10.1021/bi0523106 CCC: $33.50
Published on Web 06/03/2006

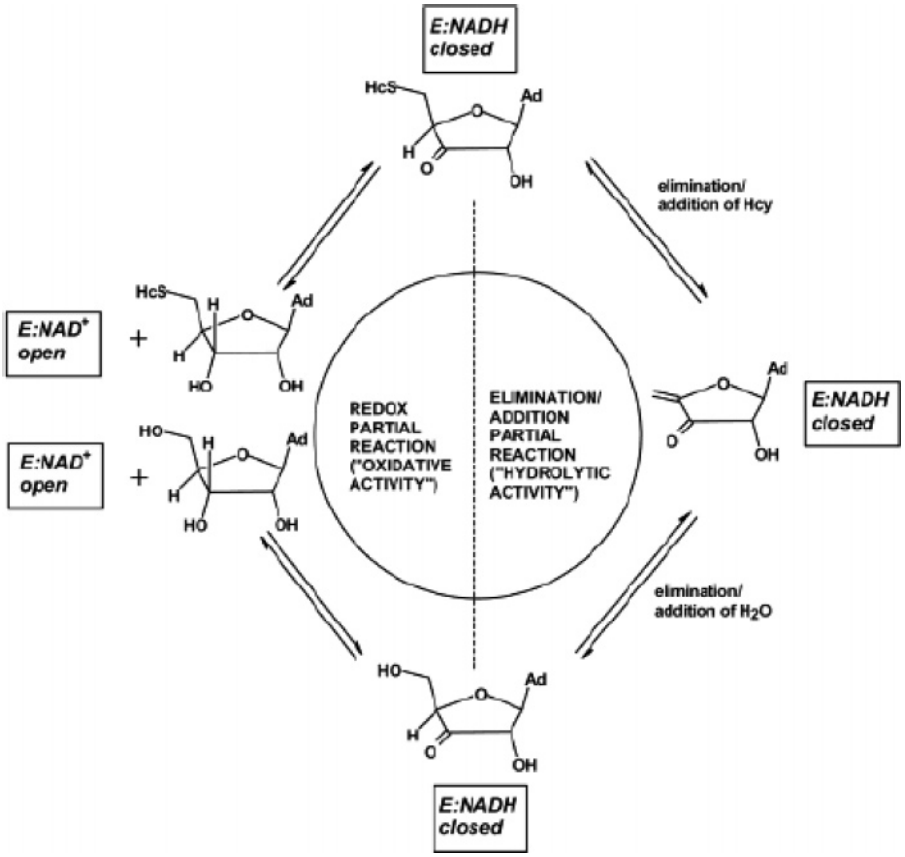

FIGURE 1: Catalytic cycle of AdoHcy hydrolase involves a redox partial reaction and an elimination/addition partial reaction (modified from ref *14*).

presence of vibrations along the open−closed conformational transition. In contrast, the low-frequency vibrations of the closed form involved coupled motions of the different subunits, suggesting the presence of a mechanical coupling between the subunits that could explain the enzyme cooperativity (*3*).

The experimental and computational results thus indicate that in the absence of the substrate the enzyme exists in the mobile open form, with each subunit executing hinge-bending motions. Binding of the substrate/inhibitor stabilizes the enzyme in the closed conformation, closing the interdomain cleft and sequestering the active site from the solvent. Rather than being completely abolished, the hinge bending/cleft opening may continue in the complex on a longer time scale, because AdoHcy hydrolase binds the substrate, catalyzes chemical conversions, and releases the product.

The hinge-bending motion thus has an important functional role, related to substrate binding, sequestering reactive intermediates in the active site and product release. To probe this motion and the roles of hinge-region residues, we have undertaken several mutagenesis studies. Several residues in HR1: Asn 181, Lys 186, Asp 190, and Asn 191 are part of the active site, and their mutations led to a dramatic decrease in catalytic activity (*8*). Additionally, eight single site-directed mutants (M351P, H353A, H353F, P354A, F356A, T363A, T363P, and M367A) were created in the HR2 and neighboring residues (*3*, *9*). Four of these mutants, M351P, H353A, P354A, and M367A, retained the quaternary structure of the wild type (WT). The remaining four, H353F, F356A, T363A, and T363P, were mixtures of dimers and tetramers, while T363P additionally exhibited the loss of secondary structure. Kinetically, the catalytic activities of all of these eight mutants, except T363P and H353F, were reduced by less than 10-fold compared to the WT. This corresponds to differences of below 1.5 kcal/mol between corresponding kinetic and thermodynamic states of the WT and mutants.

The goal of this work is to use fluorescence anisotropy measurements to probe the influence of HR2 residues on the hinge-bending motion of AdoHcy hydrolase. Three HR2 mutants, M351P, H353A, and P354A, were selected for these studies, because these proteins retain the WT quaternary structure, enzymatic activity, and ligand-binding affinities (*9*). The three selected mutants exhibited enzymatic activity differing less than 4-fold from the WT enzyme (thermodynamic difference of 0.8 kcal/mol). In this work, the WT protein and the three hinge-region mutants M351P, H353A, and P354A underwent the same labeling procedure as described previously (*7*), with the fluorophore pyrene−maleimide covalently bound to the two cysteines on the protein. For each protein, fluorescence anisotropy decays were collected using time-domain measurements from the substrate-free form and three complexes, generated upon the binding of adenosine (Ado), 3′-deoxyadenosine (3′-deoxyAdo), and neplanocin A (NepA), representing intermediates at different stages of the enzymatic cycle. The results were used to probe the role of different HR2 residues in the hinge-bending motion and the connection between hinge flexibility and protein function.

MATERIALS AND METHODS

Materials. 3′-DeoxyAdo, 5,5′-dithiobis-2-nitrobenzoic acid (DTNB), dithiothreitol (DTT), and NAD^+ were obtained

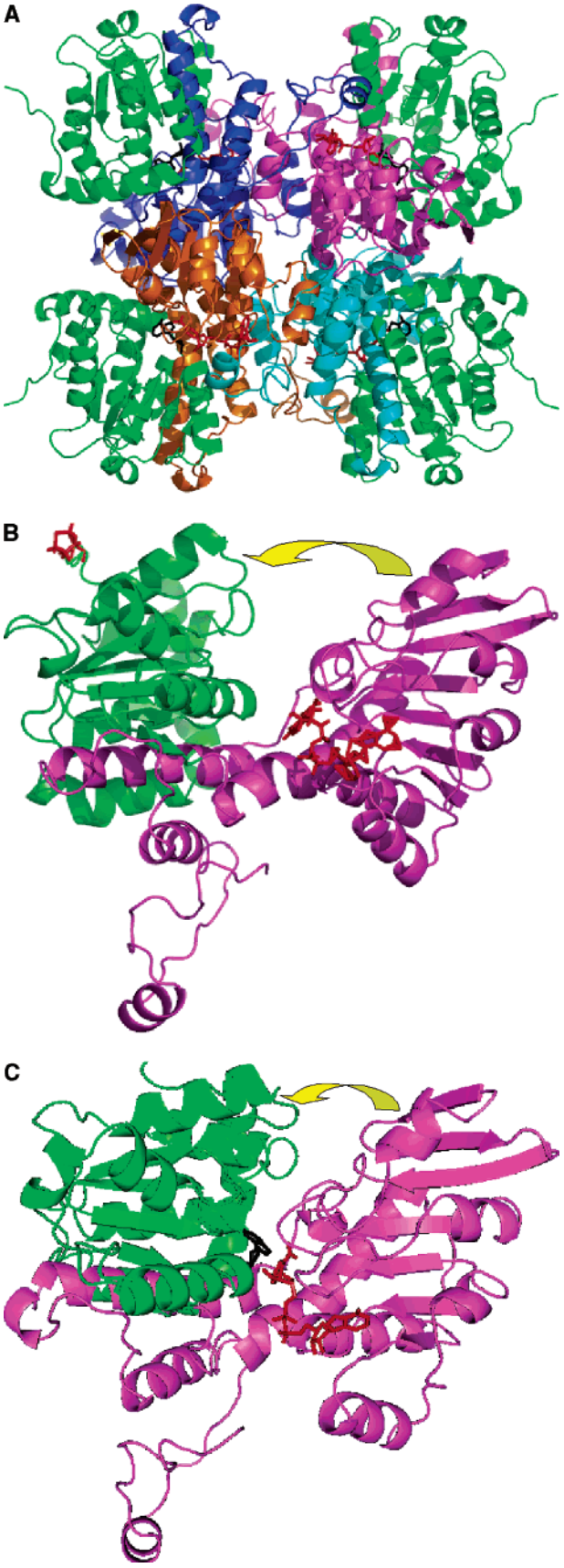

FIGURE 2: Structure of AdoHcy hydrolase. (A) Tetramer with subunits shown in different colors. (B) Monomer in the open state (*3*). (C) Monomer in the closed state (*4*). Red, cofactor; black, inhibitor.

from Sigma (St. Louis, MO). *N*-(1-pyrenyl)maleimide (PMal) was obtained from Molecular Probes (Eugene, OR). NepA was obtained from Diazyme Laboratories (La Jolla, CA). Purification and reconstitution of recombinant human placental AdoHcy hydrolase to the NAD^+ form were previously described by Elrod and co-workers (*8*). Samples were prepared in 50 mM potassium phosphate buffer (pH 7.2) with 1.0 mM ethylenediaminetetraacetic acid (EDTA).

Enzymatic Assays. The detailed protocol for AdoHcy hydrolase activity assays was described previously (*8*). In both the overall synthetic direction and the hydrolytic direction, the rate of AdoHcy formation from Ado and Hcy or the formation rate of Ado coupled with the Ado deaminase reaction from AdoHcy in buffer A [50 mM potassium phosphate (pH 7.2) with 1.0 mM EDTA] at 37 °C was measured using a C18 reversed-phase HPLC column (Vydac, Hesperia, CA). The protein concentration was measured using the Bradford assay with bovine serum albumin as a standard (*10*).

Chemical Derivatization of AdoHcy Hydrolase. AdoHcy hydrolase (0.3 mg/mL) was incubated with 12 μM PMal in the presence of 1 mM Ado in buffer A at 25 °C for 2 h, essentially as previously described by Yuan and co-workers (*11*). The reaction was quenched by the addition of 0.1 mM DTT. The unbound PMal was removed from the solution by using a Sephadex G-25 column (45 × 2.5 cm). To remove enzyme-bound Ado, the eluted protein was dialyzed against buffer A at 4 °C. Incorporation of PMal was determined using the molar extinction coefficient ϵ_{338}(PMal) = 40 000 M^{-1} cm^{-1} (*7*).

Time-Resolved Anisotropy. The time-resolved anisotropy data were collected using the method of time-correlated single-photon counting. The instrumental setup has been described previously (*12*). Briefly, a DCM (Exciton, Dayton, OH) dye laser was synchronously pumped by a mode-locked, frequency-doubled Nd:YAG laser. This laser was cavity-dumped at a rate of approximately 1.5 MHz to allow for the long fluorescence decay of PMal. The output of this laser at 680 nm was frequency-doubled to 340 nm for all experiments described here. The sample was excited approximately 1 mm from the surface of the cell to minimize absorption of emitted photons and subsequent contamination of the anisotropy decay. Fluorescence was collected at a right angle to the excitation. Decays were collected with polarizations perpendicular and parallel to the vertically polarized excitation. Normalization of such decays was accomplished by the tail-matching method: each decay was collected to the same integrated counts in a long time-scale region where rotational effects are negligible.

The anisotropy decays were calculated by the equation

$$r(\tau) = \frac{I_{||}(\tau) - I_{\perp}(\tau)}{I_{||}(\tau) + 2I_{\perp}(\tau)}$$

Because the time scales of interest in this experiment (>1 ns) are much longer that the full-width half-maximum of the instrument (100 ps), the excitation function can be well-approximated by a delta function and there was no need to account for convolution effects. Therefore, the anisotropy decays were fit to sums of exponentials using nonlinear least squares. The data were collected in time bins of approximately 0.4 ns. This bin size led to uncertainty in the fast rotational correlation times on the order of 1 ns. However, the physical phenomena observed here take place

on the time regime of 5−100 ns, and therefore, the faster time scale (≤1 ns) is not crucial for fitting the data.

Error estimates in the fitting parameters were determined using support plane analysis (*13*). This analysis fixes the parameter of interest at various values surrounding its minimum and varies all others to create a χ^2 surface for that parameter. The error limits at one standard deviation were then determined by the increase in χ^2 specified by the *F* statistic. The *F* test also provided a statistical means to determine the percent confidence in addition to a third exponential in the analysis of anisotropy decays. We considered the addition of a third component to be justified if this confidence level was above 70%.

RESULTS

Covalent Modification of WT AdoHcy Hydrolase and Mutants with PMal. AdoHcy hydrolase WT and mutants M351P, H353A, and P354A were labeled with PMal following the protocol described in the Materials and Methods. The oxidative and hydrolytic activities of AdoHcy hydrolase WT and mutants were retained following covalent modification with PMal, permitting the measurement of catalytically important global conformational changes associated with substrate binding and oxidation. A total of 1.5 ± 0.2 mol of PMal are incorporated per mole of subunit for WT and three mutants, which is consistent with previous work (*7*). Previous studies showed that of the 10 cysteine residues of AdoHcy hydrolase, only 3 sites, C113, C195, and C421, can be chemically modified using sulfhydryl-specific reagents (*11*). Proteolytic digestion and mass spectrometry have been used to prove that our derivatization protocol leads to PMal labeling at two sites, Cys113 and Cys421, in the WT protein (*7*). We have previously used circular dichroism, chromatography, and kinetics studies to show that the M351P, H353A, and P354A mutant proteins retained secondary structure, quaternary structure, enzymatic activity, and ligand affinity of the WT (*9*). When these conditions are taken together with the identical PMal incorporation ratios of the mutants and WT, they lead us to assume that the same residues C113 and C421, which were identified as labeling sites of the WT (*7*) were labeled with PMal in the mutant proteins as well.

Fluorescence Lifetimes of PMal Bound to AdoHcy Hydrolase. The fluorescence intensity decays were complex and required four exponential components to describe the fluorescence decay. This complexity may result from different environments of the two labeling sites on the protein and the complex photophysics of PMal. The lifetimes and amplitudes for the native enzyme did not differ significantly from those of Yin and co-workers (*7*). Lifetime and amplitude values for the mutants differed only slightly from those of the native enzyme for all conditions studied.

Fluorescence Anisotropy Decay: WT. The results of the time-resolved fluorescence anisotropy studies of PMal covalently bound to the WT and mutant enzymes are presented in Tables 1−4 and Figures 3−6. The tables have entries for the free enzyme with oxidized cofactor, E/NAD$^+$, and complexes resulting from the treatment of E/NAD$^+$ with three ligands. Treatment of the free enzyme with adenosine produces an equilibrium of E/NAD$^+$/Ado and E/NADH/3′-ketoAdo complexes; treatment with the unoxidizable substrate analogue 3′-deoxyAdo leads to the formation of E/NAD$^+$/3′-deoxyAdo complexes; and treatment of the free enzyme with NepA produces complexes with the oxidized ligand, E/NADH/3′-keto-NepA.

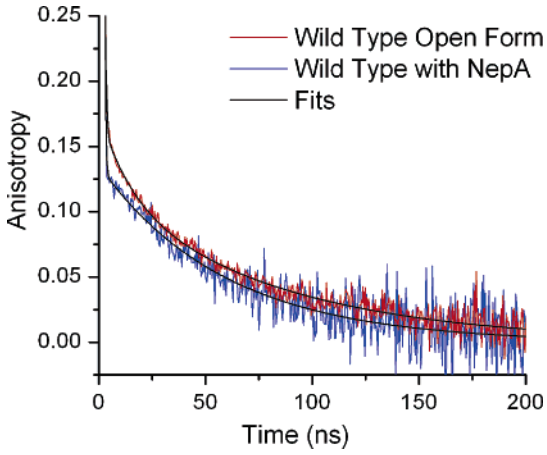

FIGURE 3: Time-resolved fluorescence anisotropy data. WT enzyme in substrate-free (open) form (red) and in the presence of NepA (blue). Fits shown as solid black lines.

For the WT enzyme in the substrate-free state and in the presence of Ado and 3′-deoxyAdo, the anisotropy decays exhibit two rotational components in addition to a short, unresolved component. Following Yin and co-workers (*7*), we assign the longest component to the overall tumbling of the protein and the intermediate component to the domain motion of AdoHcy hydrolase. The long rotational component has a correlation time of 82, 62, and 97 ns for the free enzyme and in the presence of Ado and 3′-dexyAdo, respectively. The corresponding values of the intermediate rotational component are 14, 7, and 19 ns, respectively (Table 1). The confidence level for the addition of the intermediate rotational time is above 99%. Binding of NepA, which produces the E/NADH/3′-keto-NepA complex, eliminated the intermediate rotational correlation time for the WT, with the complex exhibiting a 59 ns anisotropy decay.

The previous study of the WT protein by Yin and co-workers reported a 25 ns intermediate and 91−131 ns long correlation times (*7*), systematically higher than decay times found in our work. Also, the previous study did not observe an intermediate rotational correlation time for the WT enzyme with any inhibitors (*7*). These differences may simply reflect the enhanced sensitivity and time resolution of the present method (see χ^2 values in Table 3 of ref *7*).

Fluorescence Anisotropy Decay: M351P and P354A. The anisotropy decays for the M351P and P354A mutants, presented in Tables 2 and 3 and Figures 4 and 5, are qualitatively similar to the WT results. P354A exhibits intermediate components of 17−18 ns and long components of 96−97 ns for the free enzyme and in the presence of Ado and 3′-deoxyAdo. In M351P, intermediate components are found only in the free enzyme (14 ns) and in the presence of 3′-deoxyAdo (10 ns), with corresponding long correlation times of 88 and 97 ns. In the presence of Ado, the intermediate correlation time is missing and the long time is 84 ns (although it is possible to fit a third component, its confidence is only 56%, much lower than for the WT; Table 2). Binding of NepA eliminated or slowed the intermediate component of both M351P and P354A mutants, yielding long

Table 1: Rotational Times and Amplitudes of Native AdoHcy Hydrolase Labeled with PMal[a]

sample	r_1	ϕ_1 (ns)	r_2	ϕ_2 (ns)	r_3	ϕ_3 (ns)	χ^2	percent confidence in the third exponent[b]
E_{NAD^+}	0.13 (0.03−0.18)[c]	0.5 (0.3−0.8)	0.05 (0.03−0.09)	14 (5−31)	0.11 (0.06−0.13)	82 (69−124)	1.05	>99
E_{NAD^+}/E_{NADH} +Ado/3′-ketoAdo	0.10 (0.07−0.14)	0.5 (0.4−1.0)	0.03 (0.02−0.07)	7 (3−28)	0.12 (0.06−0.12)	62 (55−93)	1.00	99
E_{NAD^+} + 3′-deoxyAdo	0.02 (0.01−0.03)	1.4 (0.6−2.8)	0.05 (0.04−0.07)	19 (12−31)	0.11 (0.09−0.13)	97 (87−116)	1.01	99
E_{NAD^+} + 3′-ketoNepA	0.20 (0.19−0.2)	0.3 (0.3−0.4)			0.13 (0.13−0.13)	59 (54−65)	1.10	NA[d]

[a] Parameters are derived from nonlinear least-squares fits to the anisotropy decay calculated from decays collected parallel and perpendicular to the excitation polarization. The fitting function is $r(t) = \sum_i r_i \exp(-t/\phi_i)$. Samples are in 50 mM potassium phosphate buffer (pH 7.2) with 1.0 mM EDTA. [b] Confidence is assessed by a comparison of two and three exponential fits by the *F* test. [c] Error limits in each parameter are estimated at one standard deviation by support plane analysis using the *F* statistic (*13*). [d] The data set could not be fit to a unique third exponential.

Table 2: Rotational Times and Amplitudes of M351P Labeled with PMal[a]

sample	r_1	ϕ_1 (ns)	r_2	ϕ_2 (ns)	r_3	ϕ_3 (ns)	χ^2	percent confidence in the third exponent[b]
E_{NAD^+}	0.09 (0.07−0.04)	0.8 (0.5−1.3)	0.07 (0.05−0.09)	14 (8−23)	0.09 (0.06−0.11)	88 (72−124)	1.05	>99
E_{NAD^+}/E_{NADH} + Ado/3′-ketoAdo	0.03 (0.02−0.03)	2.3 (1.3−4.2)			0.17 (0.17−0.17)	84 (81−88)	0.98	56
E_{NAD^+} + 3′-deoxyAdo	0.01 (0.00−0.02)	0.9 (0.0−4.7)	0.03 (0.01−0.03)	10 (6−28)	0.15 (0.14−0.16)	97 (92−105)	1.01	70
E_{NAD^+} + 3′-ketoNepA	0.18 (0.15−0.22)	0.4 (0.3−0.4)			0.13 (0.13−0.13)	50 (47−52)	1.05	64
third exponential fit	0.19	0.4	0.07	33	0.06	72	1.03	

[a] Conditions and fitting procedures are the same as in Table 1. [b] Confidence is assessed by a comparison of two and three exponential fits by the *F* test.

Table 3: Rotational Times and Amplitudes of P354A Labeled with PMal[a]

sample	r_1	ϕ_1 (ns)	r_2	ϕ_2 (ns)	r_3	ϕ_3 (ns)	χ^2	percent confidence in the third exponent[b]
E_{NAD^+}	0.11 (0.07−0.15)	0.5 (0.3−0.8)	0.06 (0.05−0.08)	17 (11−24)	0.11 (0.09−0.13)	97 (86−114)	1.13	>99
E_{NAD^+}/E_{NADH} + Ado/3′-ketoAdo	0.02 (0.01−0.03)	1.2 (0.4−3.0)	0.03 (0.02−0.06)	18 (8−42)	0.15 (0.11−0.16)	96 (88−114)	1.01	92
E_{NAD^+} + 3′-deoxyAdo	0.03 (0.02−0.04)	1.7 (0.7−3.7)	0.05 (0.04−0.07)	17 (10−30)	0.12 (0.10−0.13)	96 (88−113)	1.07	97
E_{NAD^+} + 3′-ketoNepA	0.04 (0.03−0.04)	2.8 (1.4−3.7)			0.15 (0.15−0.16)	55 (53−58)	1.01	54
third exponential fit	0.03	1.8	0.05	28	0.11	68	0.95	

[a] Conditions and fitting procedures are the same as in Table 1. [b] Confidence is assessed by a comparison of two and three exponential fits by the *F* test.

correlation times of 50−55 ns, similar to the 59 ns value found for the WT.

For M351P and P354A in the presence of NepA, fits with three anisotropy decay components indicated a possible intermediate correlation time of ∼30 ns (Tables 2 and 3) but with lower confidence than with the free protein or in the presence of 3′-deoxyAdo. The similarity of the anisotropy decays of the NepA complexes of the WT, M351P, and P354A suggest either that the domain motion is absent in these cases or that it is present but slowed considerably. For the P354A mutant, the confidence level for the addition of the third component is above 90% for the enzyme in the substrate-free state and in the presence of Ado and 3′-deoxyAdo. In M351P, this confidence level is above 99% for the free protein and 56% in the presence of 3′-deoxyAdo.

Fluorescence Anisotropy Decay: H353A. The anisotropy decay pattern of the H353A mutant is qualitatively different from the WT and the other two mutants (Table 4 and Figure 6). In contrast to the other systems, an intermediate rotational component is not justified in H353A under any of the solution conditions studied here. H353A exhibits a correlation time of 55 ns in the substrate-free state, 58 ns with Ado, 71 ns with 3′-ketoAdo, and 70 ns with NepA. For this mutant, the free enzyme reorientations are faster and the reorientations of the NepA complex are slower than in any of the other studied systems.

DISCUSSION

Nanosecond Domain Motion of AdoHcy Hydrolase Ceases upon Binding and Oxidation of the Substrate. For WT AdoHcy hydrolase, the substrate-free form had three rotational correlation times: 0.5, 14, and 82 ns (Table 1). In accordance with a previous interpretation (*7*), we assign the short component (0.5 ns) to segmental rotational dynamics of the pyrene chromophore, the intermediate component (14 ns) to domain reorientations, and the longest component (82

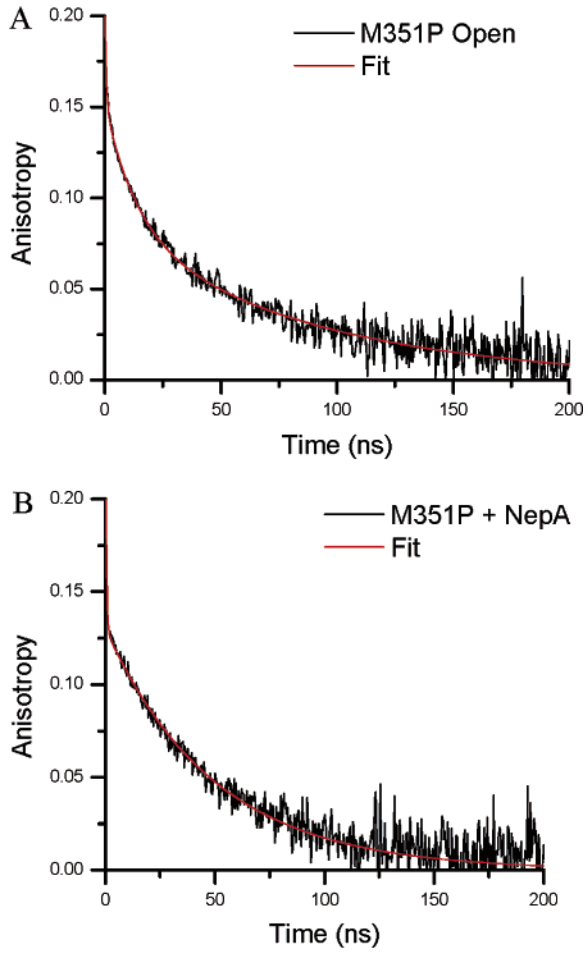

FIGURE 4: Time-resolved fluorescence anisotropy data. M351P mutant in substrate-free form (A) and in the presence of NepA (B). Data, black; fits, red.

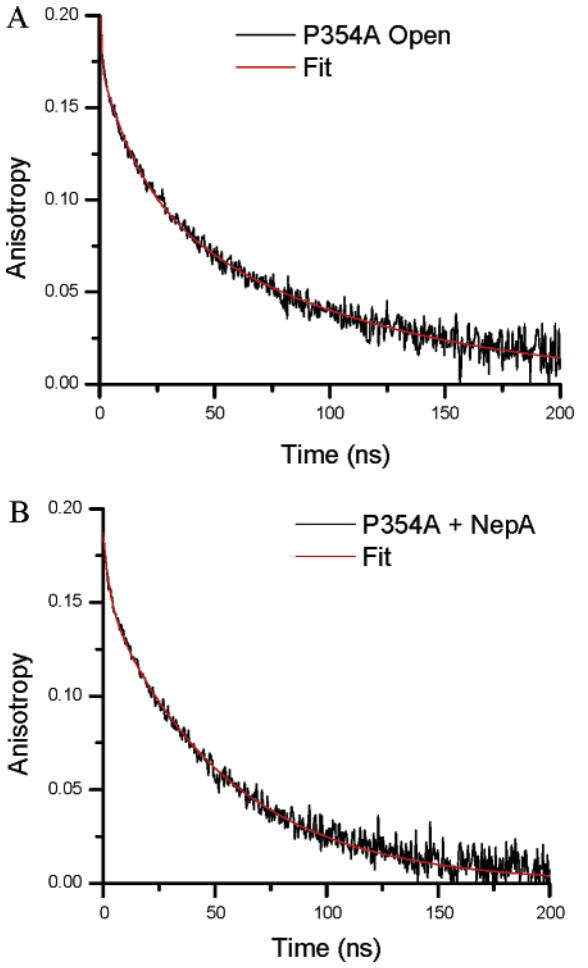

FIGURE 5: Time-resolved fluorescence anisotropy data. P354A mutant in substrate-free form (A) and in the presence of NepA (B). Data, black; fits, red.

ns) to the overall tumbling of the tetrameric AdoHcy hydrolase. On the basis of our normal-mode analysis studies, the short component may also include effects of hinge-bending vibrations occurring on a time scale of tens of picoseconds (*3*). Three rotational correlation times were also detected in the presence of the substrate Ado and the unoxidizable substrate analogue 3′-deoxyAdo, but only two, the short and long ones, were detected in the presence of NepA.

Our normal-mode analysis indicates the presence of local fluctuations at tens of picoseconds around both the open and closed structures (*3*), while this and previous fluorescence studies indicate the presence of domain reorientations at tens of nanoseconds. A straightforward interpretation of the observed pattern of correlation times is to assume that the enzyme in solution exists in an equilibrium of two states, open and closed, as observed in the crystal structures. The open form is taken to be rotationally mobile, executing domain hinge-bending fluctuations that are observed as the intermediate anisotropy decay time, while in the closed form, these motions are absent. In an alternative model, domains undergo only small local vibrations in both open and closed states [time scale of tens of picoseconds and amplitude of about 1° (*3*)] and the middle anisotropy decay is due to domain reorientations associated with the transitions between the two forms. At this point, differentiating between the two models for the middle anisotropy component is not possible. To do this, the rate of exchange between the open and closed states should be obtained from an experiment that is insensitive to the dynamics of the individual states themselves. The 10−20 ns motion is related to domain reorientations in both models, but it is a fluctuation around a single equilibrium state in one case and a transition between two stable states in the other.

One way of visualizing anisotropy parameters is by modeling restricted reorientational motion as the reorientation within a cone (*12*). The cone angle can be determined from the parameter $\beta = (1/4)\cos^2\theta(1 + \cos\theta)^2$, where β is the normalized amplitude of the long rotational component and θ is the half-angle of the cone describing the range of rotation. For the analysis of the domain rotational motion of our samples, we normalized the slow rotational amplitude with the sum of the intermediate and slow rotational amplitudes to obtain the cone angle for the domain motion. The cone angles for all samples displaying domain motion were identical within error limits. The average β value is 0.72, corresponding to an average cone half-angle θ of 26°. This is similar to the 17−19° domain reorientation between the open and closed forms of AdoHcy hydrolase found in the crystal structures (*3*). It must be noted, however, that this analysis assumes that all fluorophores contribute equally to the intermediate rotational correlation time. It may be that one of the two labeling sites is more sensitive to this motion than the other site. In that case, the cone half-angle reported

Table 4: Rotational Times and Amplitudes of H353A Labeled with PMal[a]

sample	r_1	ϕ_1 (ns)	r_2	ϕ_2 (ns)	r_3	ϕ_3 (ns)	χ^2	percent confidence in the third exponent[b]
E_{NAD^+}	0.04 (0.03−0.05)	1.6 (1.2−2.2)			0.13 (0.13−0.13)	55 (52−58)	0.91	NA[c]
E_{NAD^+}/E_{NADH} + Ado/3′-ketoAdo	0.07 (0.06−0.08)	1.3 (1.0−1.8)			0.14 (0.14−0.14)	58 (55−61)	1.13	NA[c]
E_{NAD^+} + 3′-deoxyAdo	0.04 (0.03−0.05)	1.6 (1.1−2.1)			0.15 (0.15−0.15)	71 (68−74)	1.08	50
E_{NAD^+} + 3′-ketoNepA	0.05 (0.04−0.06)	2.4 (1.9−3.1)			0.15 (0.15−0.15)	70 (67−74)	1.01	NA[c]

[a] Conditions and fitting procedures are the same as in Table 1. [b] Confidence is assessed by a comparison of two and three exponential fits by the *F* test. [c] The data set could not be fit to a unique third exponential.

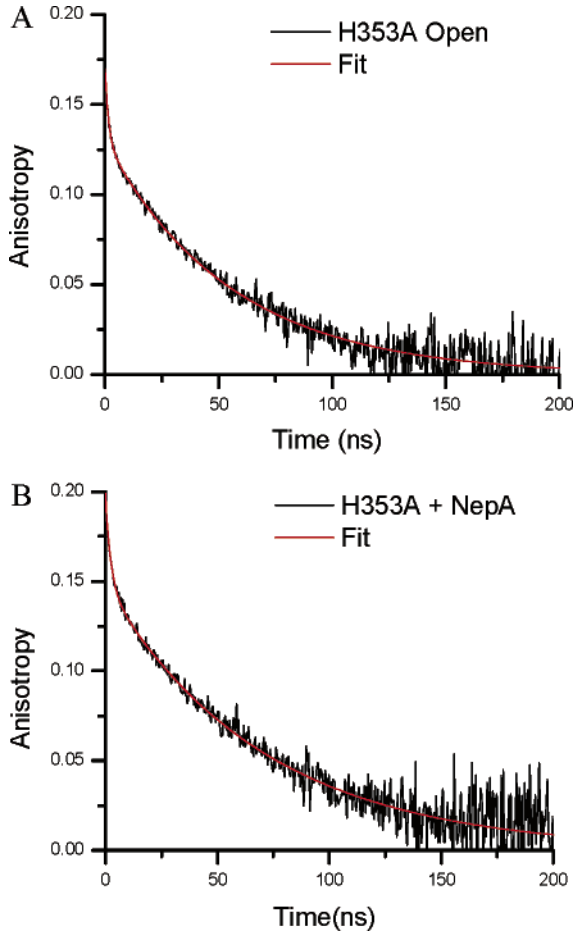

FIGURE 6: Time-resolved fluorescence anisotropy data. H353A mutant in substrate-free form (A) and in the presence of NepA (B). Data, black; fits, red.

here represents a weighted average of the motions of labels at the two sites, and the actual amplitude of motion may be greater for fluorophores at the site more sensitive to the motion.

In the presence of the substrate Ado and its nonoxidizable analogue, 3′-deoxyAdo, the WT enzyme domain motions were not abolished. In contrast, the anisotropy decay of the NepA complex with the WT enzyme was described by only two components: 0.2 and 59 ns (Table 1), consistent with results of Yin et al. (*7*). After binding, the strong inhibitor NepA is oxidized at the 3′ position of the cyclopentenyl ring to form the 3′-keto derivative with concomitant conversion of the enzyme from the NAD^+ to the NADH form. This state is an analogue of the central catalytic intermediate of the enzymatic cycle [Figure 1 (*14*)]. The observed pattern of presence of the intermediate components suggests that domain motions and the hydrodynamic properties of the enzyme−ligand complex are not significantly altered at the ligand-binding stage, and it is ligand oxidation that results in global structural change within the AdoHcy hydrolase tetramer, locking the enzyme in its closed conformation. The absence of the intermediate anisotropy decay component upon binding of NepA suggests that domain motions within AdoHcy hydrolase are substantially reduced or eliminated following substrate binding and oxidation. Alternatively, the motion may still occur but on a time scale outside the 0.1−200 ns range accessible in our experiments.

M351P and P354A Mutations Have a Minimal Effect on Domain Motion. The anisotropy decays of the mutants M351P (Table 2) and P354A (Table 3) were similar to the WT. M351P and P354A exhibited three decay components in the absence of the substrate and in the presence of 3′-deoxyAdo and two or three decay components in the presence of NepA. The M351P and P354A middle components were in the 10−18 ns range, showing a strong overlap with the 7−19 ns range found for the WT. The long correlation times were in the 50−55 ns range for the M351P and P354A mutants in the presence of NepA and 84−97 ns in the other ligation states (Tables 2 and 3), comparable to the corresponding values of the WT, 59 and 62−97 ns, respectively. Thus, the pattern of decay times indicates that the WT and M351P and P354A mutants have similar hydrodynamic parameters and that they exhibit similar domain motions, which are not markedly affected by ligand binding alone, while being eliminated or significantly slowed by binding and oxidation of NepA. The fit for M351P with Ado suggests a possible intermediate component, as with the native enzyme and P354A, but it was not as well-resolved. M351P and P354A are two opposite mutations in the sense of rigidity, with the former expected to make the hinge more rigid and the latter expected to make it more flexible. The fact that these mutations did not lead to marked changes in the observed domain motions indicates that the conformational flexibility of residues 351 and 354 is not important for hinge dynamics in AdoHcy hydrolase.

The H353A Mutation Significantly Affects Hinge-Bending Motion. The pattern of rotational correlation times of the H353A mutant was markedly different from those observed in the other systems (Table 4). Most strikingly, the intermediate decay time was not found for the substrate-free enzyme or for any of the three ligand complexes. At the same time, the H353A system exhibited the lowest value of

the long correlation time in the substrate-free state and the highest value of this correlation time in the presence of NepA among the studied forms of the hydrolase. This can be interpreted in two ways. One possibility is that the mutation slows down the domain motions to about 50 ns, leading to an approximate coincidence of the time scales of domain reorientation and overall tumbling, reflected as an observation of a single effective correlation time of 55−70 ns (see below). Another possibility is that the H353A mutation induces a global conformational change, decreasing the hydrodynamic size of the open form and increasing the size of the closed form. It is possible that a combination of both effects occurs, i.e., slowing down the domain motions and changing the enzyme shape/size. Slowing down the domain reorientation and associated cleft opening/closing should not measurably affect the enzymatic activity until the time scale of enzyme turnover is reached, i.e., ca. 1 s (*15*).

Although mutations could slow domain movements, the time scale of the motion is in the nanosecond range, while the catalytic turnover rate is of the order of 1 s. Thus, the extent of slowing down the motion was not enough to be rate-limiting. The slower binding of the substrate, on the other hand, could be due to a slower domain motion in mutants. Overall, the HR2 is important in structure and motion but is not directly involved in the catalytic activity. The hinge can affect the activity by holding the substrate and cofactor in position.

Analysis of the Third Anisotropy Decay Component. The longest rotational correlation time is assigned to the overall tumbling of the tetrameric protein in solution. Hydrodynamic calculations using HYDROPRO (*16*) predicted rotational correlation times for the different molecular axes between 122 and 134 ns (average of 128 ns) for the tetramer in the open form (PDB file 1B3R) and between 95 and 111 ns (average of 103 ns) for the closed form (tetramer constructed from PDB file 1A7A) (*7*). These calculations assumed a rigid body moving in a continuous medium. For AdoHcy hydrolase, we can rationalize the differences between the hydrodynamic and fluorescence rotational correlation times by the presence of domain motions and possibly differential solvation of the open and closed conformers (*17*).

The crystallographic data suggest that the equilibrium is shifted toward the open form in the absence of the substrate and toward the closed form after the addition of substrates/analogues. On the basis of the hydrodynamic calculations, we expect the closed form to tumble approximately 30% faster than the open form. Using the data for the WT and M351P and P354A mutants, which showed similar patterns and values of correlation times, it is plausible to assign the higher observed values of the long anisotropy decay component, 82−97 ns, to the tumbling of the open form, and the lower values, 50−62 ns, to the closed form. The error limits for the closed states, which exhibited two-exponential decay, are small compared to those for the three exponential data fits and, in many cases, are much less than would be expected if an unresolved rotational time at 90 ns existed. Therefore, it seems likely that the reduction in the correlation time is due to changes in the size and shape. The pattern of long anisotropy decay components in Tables 1−3 would then be consistent with the protein populating mostly the open structure in the absence of the substrate or in complexes with the unoxidizable 3′-deoxyAdo, mostly the closed structure in the complex with NepA, and a mixture of the two in the presence of Ado.

As discussed above, the long anisotropy decay components of the H353A mutant differ from the WT and the remaining mutants, which may be due to both changes in the time scale of domain motions and changes in the protein size and shape.

Effects of Ado Binding. In the presence of Ado, the enzyme forms an equilibrium between the E/NAD^+/Ado and E/NADH/3′-ketoAdo forms. In accordance with our discussion presented above, we should thus expect to see results intermediate between those for NepA (producing E/NADH/3′-ketoNepA) and the unoxidizable 3′-deoxyAdo (producing E/NAD^+/3′-deoxyAdo). Inspection of Tables 1−3 shows that this is mostly the case. Thus, for the WT enzyme, adding Ado does not eliminate the middle anisotropy component, while the long anisotropy component, 62 ns, is significantly lower than the 97 ns found in the 3′-deoxyAdo complex, suggesting that both open and closed conformations of the hydrolase are populated. For M351P in the presence of Ado, the intermediate decay component was not observed, while the long component was 84 ns, somewhat lower than with 3′-deoxyAdo (97 ns) but comparable to the substrate-free form (88 ns). As discussed above, the fit for M351P with Ado suggests a possibility of the presence of an intermediate decay component but with a lower confidence than in the free enzyme. The observed pattern of correlation times could then be explained by the shift in the equilibrium toward a predominance of the closed confomer for this mutant. In the case of P354A, the correlation times are essentially identical for the substrate-free enzyme and with Ado and 3′-ketoAdo, suggesting that in these ligation states the mutant exists primarily in the open form (Table 3). Thus, the fluorescence data suggest that the M351P and P354A mutations influence the equilibrium between the open and closed conformers of the hydrolase. For H353A, we hypothesize a change in the domain-motion rate and protein shape/size compared to the WT. For this mutant, the long correlation time in the presence of Ado, 58 ns, is most similar to the value found for the free enzyme, 55 ns (Table 4), while adding either 3′-deoxyAdo or NepA yields times of 70−71 ns. This pattern is markedly different than observed in the other systems studied.

CONCLUSIONS

We have performed fluorescence anisotropy decay studies to follow the structure and dynamics of AdoHcy hydrolase in its catalytic cycle. To investigate the roles of residues in HR2 (residues 351−356), the WT and three catalytically active mutants of the enzyme, M351P, P354A, and H353A, were fluorescently labeled with PMal. To probe changes of the structure and dynamics at different stages of the enzymatic reaction, we studied the substrate-free enzyme and complexes of the enzyme with Ado, 3′-deoxyAdo, and NepA. In the absence of the substrate, the WT enzyme exhibited three rotational correlation times: 0.5 ns, assigned to local chromophore reorientations and protein vibrations, 14 ns, assigned to domain reorientations, and 82 ns, assigned to the overall protein tumbling in solution. Protein complexes with 3′-deoxyAdo, which correspond to either early enzymatic cycle stages after substrate binding or late stages prior to product release, exhibited similar three-component ani-

sotropy decays. In contrast, binding the strong inhibitor NepA, which is an analogue of the central catalytic intermediate (*14*), led to the elimination of the middle correlation time and shortening of the long time. In turn, binding Ado produces an equilibrium between complexes corresponding to early/late and central catalytic intermediates, exhibiting fluorescence with properties of both states, with the presence of the intermediate decay, although at a lower amplitude than in the free enzyme, and shortening of the long decay to a value between those of the free enzyme and NepA complexes.

The anisotropy results, together with previous crystallographic studies, indicate that AdoHcy hydrolase exists in an equilibrium between open and closed structures, with the equilibrium shifted toward the open form for the substrate-free enzyme and shifted toward the closed form in the presence of substrates/analogues. Thus, we assign the largest values of the long correlation time, 82−97 ns for the WT, to the tumbling of the open form, and the shorter values, 59−62 ns for the WT, to the tumbling of the more compact closed form. The fluorescence results indicate that the enzyme undergoes a transition to the closed form, in which the active sites are sequestered from the solvent, only during the central part of the catalytic cycle, after the substrate is both bound and oxidized. The experimental data are consistent with two models of the source of the middle anisotropy decay component. In the first model, the middle component is due to domain hinge-bending motions of a fluctuating nature that occur in the more flexible open structure and are abolished after the transition to the closed form. In the second model, the middle component is due to transitions between the open and closed forms.

Interestingly, the results for the M351P and P354A mutants were qualitatively similar to those for the WT. This indicates that large changes in flexibility at these positions did not influence the hinge-bending motions. However, the H353A mutant exhibited markedly different anisotropy decay features: elimination of the middle decay component and shortening of the longest component to 55−71 ns for all four ligation states studied. Because this mutant, like the others studied here, remains catalytically active, we interpret these effects as resulting from a combination of slowing down the hinge-bending motion (to the time scale of the overall protein tumbling or longer) and changes in the protein size and shape. Thus, we have produced a protein with a modified rate of domain motions. This exciting discovery will be the topic of further studies. Overall, we can conclude that hinge bending plays an important role in the enzymatic catalysis of AdoHcy hydrolase. The fluorescence results are consistent with a picture where a hinge bend locks the enzyme in the closed form following oxidation of the bound substrate. We are currently modeling the detailed nature of the domain motions of AdoHcy hydrolase through molecular dynamics simulations.

ACKNOWLEDGMENT

This work was supported by NIH Grant GM29332.

SUPPORTING INFORMATION AVAILABLE

Fluorescence anisotropy decays of the WT and M351P, P354A, and H353A mutants with Ado and 3′-deoxyAdo. This material is available free of charge via the Internet at http://pubs.acs.org.

REFERENCES

1. de la Haba, G., and Cantoni, G. L. (1959) The enzymatic synthesis of *S*-adenosyl-L-homocysteine from adenosine and homocysteine, *J. Biol. Chem. 234*, 603−608.
2. Yin, D., Yang, X., and Borchardt, R. T. (2000) *Biomedical Chemistry: Applying Chemincal Principles to the Understanding and Treatment of Disease*, Chapter 2, John Wiley and Sons, Inc., New York.
3. Wang, M., Borchardt, R. T., Schowen, R. L., and Kuczera, K. (2005) Domain motions and the open-to-closed conformational transition of an enzyme: A normal mode analysis of *S*-adenosyl-L-homocysteine hydrolase, *Biochemistry 44*, 7228−7239.
4. Hu, Y., Komoto, J., Huang, Y., Gomi, T., Ogawa, H., Takata, Y., Fujioka, M., and Takusagawa, F. (1999) Crystal structure of *S*-adenosylhomocysteine hydrolase from rat liver, *Biochemistry 38*, 8323−8333.
5. Turner, M. A., Yuan, C. S., Borchardt, R. T., Hershfield, M. S., Smith, G. D., and Howell, P. L. (1998) Structure determination of selenomethionyl *S*-adenosylhomocysteine hydrolase using data at a single wavelength, *Nat. Struct. Biol. 5*, 369−376.
6. Turner, M. A., Yang, X., Yin, D., Kuczera, K., Borchardt, R. T., and Howell, P. L. (2000) Structure and function of *S*-adenosylhomocysteine hydrolase, *Cell Biochem. Biophys. 33*, 101−125.
7. Yin, D., Yang, X., Hu, Y., Kuczera, K., Schowen, R. L., Borchardt, R. T., and Squier, T. C. (2000) Substrate binding stabilizes *S*-adenosylhomocysteine hydrolase in a closed conformation, *Biochemistry 39*, 9811−9818.
8. Elrod, P., Zhang, J., Yang, X., Yin, D., Hu, Y., Borchardt, R. T., and Schowen, R. L. (2002) Contributions of active site residues to the partial and overall catalytic activities of human *S*-adenosylhomocysteine hydrolase, *Biochemistry 41*, 8134−8142.
9. Wang, M. (2005) Ph.D. Thesis, Department of Molecular Biosciences, University of Kansas, Lawrence, KS.
10. Bradford, M. M. (1976) A rapid and sensitive method for the quantitation of microgram quantities of protein utilizing the principle of protein−dye binding, *Anal. Biochem. 72*, 248−254.
11. Yuan, C. S., Ault-Riche, D. B., and Borchardt, R. T. (1996) Chemical modification and site-directed mutagenesis of cysteine residues in human placental *S*-adenosylhomocysteine hydrolase, *J. Biol. Chem. 271*, 28009−28016.
12. Unruh, J. R., Gokulrangan, G., Wilson, G. S., and Johnson, C. K. (2005) Fluorescence properties of fluorescein, tetramethylrhodamine and Texas Red linked to a DNA aptamer, *Photochem. Photobiol. 81*, 682−690.
13. Johnson, M. L., and Faunt, L. M. (1992) Parameter estimation by least-squares methods, *Methods Enzymol. 210*, 1−37.
14. Yang, X., Hu, Y., Yin, D. H., Turner, M. A., Wang, M., Borchardt, R. T., Howell, P. L., Kuczera, K., and Schowen, R. L. (2003) Catalytic strategy of *S*-adenosyl-L-homocysteine hydrolase: Transition-state stabilization and the avoidance of abortive reactions, *Biochemistry 42*, 1900−1909.
15. Porter, D. J., and Boyd, F. L. (1991) Mechanism of bovine liver *S*-adenosylhomocysteine hydrolase. Steady-state and pre-steady-state kinetic analysis, *J. Biol. Chem. 266*, 21616−21625.
16. Garcia de la Torre, J., Huertas, M. L., and Carrasco, B. (2000) Calculation of hydrodynamic properties of globular proteins from their atomic-level structure, *Biophys. J. 78*, 719−730.
17. Cantor, C. R., and Schimmel, P. R. (1980) *Biophysical Chemistry, Techniques for the Study of Biological Structure and Function*, Vol. 2, W. H. Freeman, New York.

BI0523106